PHILOSOPHICAL TRANSACTIONS OF THE ROYAL SOCIETY A

CrossMark click for updates

Phil. Trans. R. Soc. A (2012) **370**, 4748–4769
doi:10.1098/rsta.2011.0355

Review

Robust dynamical decoupling

By Alexandre M. Souza, Gonzalo A. Álvarez and Dieter Suter*

Fakultät Physik, Technische Universität Dortmund, 44221 Dortmund, Germany

Quantum computers, which process information encoded in quantum mechanical systems, hold the potential to solve some of the hardest computational problems. A substantial obstacle for the further development of quantum computers is the fact that the lifetime of quantum information is usually too short to allow practical computation. A promising method for increasing the lifetime, known as dynamical decoupling (DD), consists of applying a periodic series of inversion pulses to the quantum bits. In the present review, we give an overview of this technique and compare different pulse sequences proposed earlier. We show that pulse imperfections, which are always present in experimental implementations, limit the performance of DD. The loss of coherence due to the accumulation of pulse errors can even exceed the perturbation from the environment. This effect can be largely eliminated by a judicious design of pulses and sequences. The corresponding sequences are largely immune to pulse imperfections and provide an increase of the coherence time of the system by several orders of magnitude.

Keywords: decoherence; spin dynamics; quantum computation; quantum information processing; dynamical decoupling; quantum memories

1. Introduction

During the last decade, it was shown that quantum mechanical systems have the potential for processing information more efficiently than classical systems [1–4]. However, it remains difficult to realize this potential because quantum systems are extremely sensitive to perturbations. These perturbations arise from couplings to external degrees of freedom and from the finite precision with which the systems can be realized and controlled by external fields. This loss of quantum information to the environment is called decoherence [5]. Different results show that a state is more sensitive to decoherence as the number of qubits increases [6–13]. This is also manifested by the impossibility to time reverse a quantum evolution when an initially localized excitation spreads out [14–17]. As the information is distributed over an increasing number of qubits, the evolution becomes more sensitive to perturbations [17,18]. In a similar vein, this increase of the sensitivity with the system size limits the distance over

*Author for correspondence (dieter.suter@tu-dortmund.de).

One contribution of 14 to a Theme Issue ‘Quantum information processing in NMR: theory and experiment’.

which one can transfer information or analogously limits the number of qubits that one can control reliably [19,20]. This is manifested as a localization effect for the quantum information [19–27]. In order to overcome these limitations and implement quantum information processing (QIP) with large numbers of qubits, methods for reducing decoherence have to be developed.

One can tackle the problem by correcting the errors generated by the perturbations, but this is only possible if the perturbation is small enough to keep the quantumness of the system [28–30]. Therefore, one needs first to reduce the perturbation effects. The pioneering strategies for reducing decoherence were introduced in the nuclear magnetic resonance (NMR) community, in particular by Erwin Hahn who showed that inverting a spin-$\frac{1}{2}$ system (a qubit) corresponds to an effective change of the sign of the perturbation Hamiltonian and therefore generates a time reversal of the corresponding evolution [31]. This leads to the formation of an echo that later was formalized as a Loschmidt echo [18]. These manipulations were extended to the so-called decoupling methods [32–36], which disconnect effectively the environment.

In the context of this review, we describe the environment as a spin-bath, without loss of generality. Considering spins 1/2 as qubits, two different types of decoupling methods can be distinguished. In the first case, the qubit system is well distinguished from the environment. Its energy level splitting differs significantly from that of the bath. As a result, the coupling between them is much smaller than the difference of their energy level splittings. The interaction can then always be approximated by an Ising-type (zz) interaction, which causes dephasing of the system qubit but not qubit flips. The decoupling methods required for these cases are called heteronuclear decoupling within the NMR community and they can involve manipulation only on the spin system [31–33,35,36] or only at the environment [37].

In the second case, the system and the environment have similar energy level splittings. This is the case of a homonuclear system where the general form of the coupling must be retained and it can induce flips of the system qubit as well as dephasing. In this case, decoupling will generally affect the complete system plus 'bath' [38–43].

In this review, we focus on the heteronuclear (pure dephasing) case and apply control pulses only to the system. During the last few years, this technique has gathered a lot of interest because it requires relatively modest resources: it requires no overhead of information encoding, measurements or feedback. The method is known as dynamical decoupling (DD). Since its initial introduction [44], a lot of effort has been invested to find sequences with improved error suppression [45–54]. The optimal design of DD sequences depends on the different sources of errors. The system-environment (SE) coupling may be a pure dephasing interaction, when it commutes with the system Hamiltonian, or it may also contain non-commuting terms. Sequences like Carr–Purcell (CP) and Carr–Purcell–Meiboom–Gill (CPMG), which use rotations around a single axis, are useful when the SE coupling operators are orthogonal to the rotation axis. In the general case, where the SE interaction includes all three components (S_x, S_y and S_z), pulses along different spatial direction have to be applied. The shortest sequence that fulfils this condition is the XY-4 sequence [35,44]. An actual implementation must take into account, in addition to the earlier-mentioned issues, the effect of pulse imperfections [45,54–58]. Fighting the effect

of pulse errors was in fact the original motivation for the development of the XY-4 sequence [35]. Another experimental consideration is the amount of power deposited in the system, which often must be kept small to avoid heating effect or damage to the sample.

The DD technique is becoming an important tool for QIP [49,54–56,59–67] as well as in spectroscopy [68–71] and imaging [72–75]. In most cases, the goal is to preserve a given input state, but it may also be combined with gate operations [76–80]. Decoherence effects due to the environment can in principle be reduced by shortening the cycle time τ_c. Clearly, this procedure is limited by finite field strengths and associated pulse durations. Within these limitations, the goal remains to find those sequences that provide the best possible decoupling performance [45,54,55,67,81–84]. Furthermore, the pulses do not only have finite lengths, they also do not implement perfect rotations. Thus, increasing the number of pulses can result in a large overall error that destroys the qubit coherence instead of preserving it. As a result, the performance of the decoupling sequence may have an optimum at a finite cycle time [54,55,67].

In this review, we summarize the different DD strategies for fighting the effect of pulse imperfections and we show how they can be implemented in the design of useful DD sequences. The paper is structured as follows. In §2, we give some basics of DD, in §3, we introduce the effects of pulse imperfections and in §4, we describe the strategies to fight their effects. In the last section, we draw some conclusions and discuss perspectives for future work.

2. Basics of dynamical decoupling

(a) *The system*

We consider a single qubit $\hat{S}$ as the system that is coupled to the bath. In a resonantly rotating reference frame [85], the free evolution Hamiltonian is

$$\hat{\mathcal{H}}_{\mathrm{f}} = \hat{\mathcal{H}}_{\mathrm{SE}} + \hat{\mathcal{H}}_{\mathrm{E}}, \tag{2.1}$$

where $\hat{\mathcal{H}}_{\mathrm{E}}$ is the Hamiltonian of the environment and

$$\hat{\mathcal{H}}_{\mathrm{SE}} = \sum_{\beta} (b_z^{\beta} \hat{E}_z^{\beta} \hat{S}_z + b_y^{\beta} \hat{E}_y^{\beta} \hat{S}_y + b_x^{\beta} \hat{E}_x^{\beta} \hat{S}_x) \tag{2.2}$$

is a general interaction between the system and the environment. $\hat{E}_u^{\beta}$ are operators of the environment and b_u^{β} the SE coupling strength. The index $\boldsymbol{\beta}$ runs over all modes of the environment. Dephasing is due to an interaction that includes the z component of the spin-system operator, while the x and/or y operators cause spin-flips. A heteronuclear spin–spin interaction involves a pure dephasing interaction. This type of interaction occurs in a wide range of solid-state spin systems, including nuclear spins in NMR [32,33,55,65], electron spins in diamonds [56], electron spins in quantum dots [86], donors in silicon [87], etc. In other cases, when the system and environment have similar energy level splittings, the SE interaction can include terms along the x-, y- and z-axis.

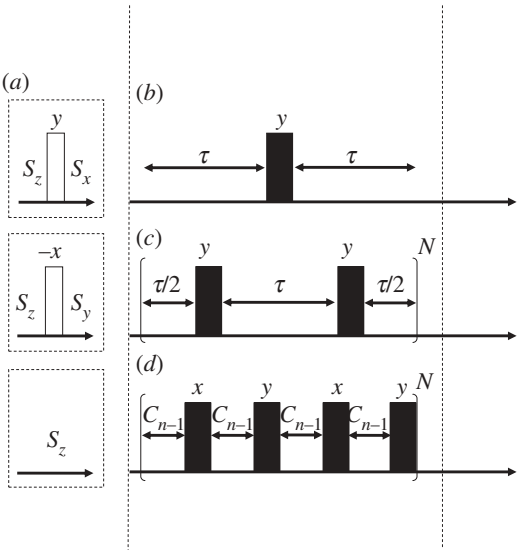

Figure 1. Dynamical decoupling pulse sequences. The empty and solid rectangles represent 90° and 180° pulses, respectively, and N represents the number of iterations of the cycle. (*a*) Initial state preparation. (*b*) Hahn spin-echo sequence. (*c*) CPMG sequence. (*d*) CDD sequence of order N, $\mathrm{CDD}_N = C_n$ and $C_0 = \tau$.

(*b*) *Dynamical decoupling sequences with a single rotation axis*

DD is achieved by iteratively applying to the system a series of stroboscopic control pulses in cycles of period τ_c [44]. Over that period, the time-averaged SE interaction can be described by an averaged or effective Hamiltonian [88]. The goal of DD is the elimination of the effective SE interaction. This can be seen by looking at Hahn's pioneering spin-echo experiment [31] (figure 1*b*). It is based on the application of a π-pulse to the spin system at a time τ after the spins were left to evolve in the magnetic field. This pulse effectively changes the sign of the SE interaction—in this case, the Zeeman interaction with the magnetic field. Letting the system evolve for a refocusing period or time reversed evolution during the same duration τ generates the echo. If the magnetic field is static, the dynamics is completely reversed and the initial state of the spin recovered. However, if the magnetic field fluctuates, its effect cannot be reversed completely. Thus, the echo amplitude decays as a function of the refocusing time [31,32]. This decay contains information about the time-dependence of the environment.

To reduce the decay rate of the echo due to a time-dependent environment, Carr and Purcell introduced a variant of the Hahn spin-echo sequence, where the single π-pulse is replaced by a series of pulses separated by intervals of duration τ [32]. This CP sequence reduces the changes induced by the environment if the pulse intervals are shorter than the correlation time of the environment. However, as the number of pulses increases, pulse errors tend to accumulate. Their combined effect can destroy the state of the system, rather than preserving it against the effect of the environment. This was noticed by Meiboom & Gill [33] who proposed a modification of the CP sequence for compensating pulse errors, the CPMG sequence.

The CP and CPMG sequences are useful only when the interaction with the environment includes not more than two of the spin operators S_x, S_y and S_z. They can be written as

$$f_{\tau/2}\,\hat{Y}\,f_{\tau}\,\hat{Y}\,f_{\tau/2}, \tag{2.3}$$

where f_τ is a free evolution operator, and $\hat{Y}$ is a π pulse around the Y-axis (and correspondingly for X). The difference between the CP and CPMG sequences is the orientation of the rotation axis with respect to the initial condition. For applications in QIP, this distinction cannot be made in general, because gate operations have to be independent of the initial condition, which must be considered unknown. CP or CPMG is the shortest sequence of pulses for decoupling an SE interaction that includes only two of the spin components S_x, S_y and S_z [44].

Usually, the average Hamiltonian generated by a DD sequence can be described by a series expansion, such as the Magnus expansion [89]. All the higher-order terms in this expansion describe imperfections, which reduce the fidelity of the sequence and should be eliminated. Improving the DD performance is therefore related to reducing the contribution of higher order terms. This is closely related to efforts for developing better decoupling sequences for NMR [34]. For QIP, this led to the design of sequences that make DD more effective, such as concatenated DD [46,81]. An important innovation was due to Uhrig [47], who proposed a sequence with non-equidistant pulse spacings, while all the standard sequences like CPMG are based on equidistant pulses. The Uhrig dynamical decoupling (UDD) sequence is defined by

$$\mathrm{UDD}_N = f_{\tau_{N+1}}\,\hat{Y}\,f_{\tau_N}\,\hat{Y}\cdots\hat{Y}\,f_{\tau_2}\,\hat{Y}\,f_{\tau_1}, \tag{2.4}$$

where the delays $\tau_i = t_i - t_{i-1}$ are determined by the positions

$$t_i = \tau_{\mathrm{c}}\sin^2\left[\frac{\pi i}{2(N+1)}\right] \tag{2.5}$$

of the pulses with $t_{N+1} = \tau_{\mathrm{c}}$ and $t_0 = 0$. The lowest non-trivial order is equal to the CPMG sequence, $\mathrm{UDD}_2 = \mathrm{CPMG}$.

The effect of the non-equidistant pulses can be discussed in the context of filter theory: DD can be considered as an environmental noise filter, where the distribution of pulses generates different filter shapes as a function of the frequencies. The overlap of this filter function with the spectral distribution of the environmental noise determines the decoherence rate [90]. Analogously, the filter shapes can be connected to diffraction patterns induced by interferences in the time domain [65]. The UDD sequence was shown theoretically to be the optimal sequence for reducing low frequency noise [47,90,91]. This prediction was confirmed experimentally [49,61,68]. However, it appears that non-equidistant sequences perform better only for particular noise spectral densities that increase for higher frequencies and have a strong cutoff. In the more frequent case, where the spectral density decreases smoothly with the frequency, equidistant sequences were predicted [90–92] and demonstrated [49,55,56,62,63,65] to be the best option [65].

This filter function description can be traced back to previous NMR approaches [93] and to work on universal dynamical control [94]. Choosing the

times for the pulses leads to a variety of sequences that can be optimized according to the spectral density of the bath [48,49,52,92,94–96].

(c) Dynamical decoupling sequences with multiple rotation axes

If the SE interaction includes all three components of the system spin operator, decoupling can only be achieved if the sequence includes rotations around at least two different axes. Such sequences are also required when the refocusing pulses have finite precision: their imperfections create an effective general SE interaction [55,67,81]. The first decoupling sequence that was introduced for this type of interaction was the XY-4 sequence, which alternates rotations around the x- and y-axes (see figure 1d, $n=1$). This sequence was initially used to eliminate the effect of pulse errors in the CP and CPMG sequences [35]. It is also the shortest sequence for DD for general SE interactions [44].

If we take pulse imperfections into account, the performance of the CP/CPMG sequence depends strongly on the initial condition. If the initial condition is oriented along the rotation axis of the pulses, flip angle errors of the first pulse are refocused by the second pulse. However, for components perpendicular to the rotation axis, the pulse errors of all pulses add and cause rapid decay of the coherence, even in the absence of SE interactions [35,55]. This motivated the development of the XY-4 sequence, which partially eliminates pulse errors over one cycle. In the QIP community, the XY-4 sequence is usually referred to as periodic DD (PDD).

The XY-4 sequence is also the building block for concatenated DD (CDD) sequences that improve the decoupling efficiency [46,81]. The CDD scheme recursively concatenates lower order sequences to increase the decoupling efficiency. The CDD evolution operator for its original version for a recursion order of N is given by

$$\mathrm{CDD}_N = C_n = \hat{Y}\, C_{n-1} \hat{X}\, C_{n-1}\, \hat{Y}\, C_{n-1} \hat{X}\, C_{n-1}, \tag{2.6}$$

where $C_0 = f_\tau$ and $\mathrm{CDD}_1 = \mathrm{XY\text{-}4}$. Figure 1 shows a general scheme for this process. Each level of concatenation reduces the norm of the first non-vanishing order term of the Magnus expansion of the previous level, provided that the norm was small enough to begin with [46,81]. This reduction comes at the expense of an extension of the cycle time by a factor of four. If the delays between the pulses are allowed to be non-equidistant like in UDD, it becomes possible to create hybrid sequences, such as CUDD [50] and QDD [53,97,98].

3. Effects of imperfections

Because the precision of any real operation is finite, the control fields used for decoupling introduce errors. Depending on the sequence, these errors can accumulate. If the number of pulses is large and the sequence is not properly designed, the accumulated pulse errors can reduce the fidelity more than the coupling to the environment. Designing effective decoupling sequences that suppress environmental effects without degrading the system, even if the control

fields have errors, requires a careful analysis of the relevant errors and appropriate strategies for combining rotations in such a way that the errors cancel rather than accumulate.

One non-ideal property of real control pulses is their finite duration, which implies a minimum achievable cycle time. The effects introduced by finite pulse lengths have been considered in different theoretical works [45,81,82]. These works predict that high order CDD or UDD sequences in general lose their advantages when the delays between the pulses or the duration of the pulses themselves are strongly constrained. While the limitation on the cycle time reduces the maximal achievable DD performance, pulse errors can be even more destructive. In most cases, the dominant cause of errors is a deviation between the ideal and the actual amplitude of the control fields. The result of this amplitude error is that the effective rotation angle deviates from π, typically by a few percent. Another important error occurs when the control field is not applied on resonance with the transition frequency of the qubit. This off-resonant effect produces a rotation in which the flip angle and the rotation axis deviate from their ideal values.

An example of the destructive effect of pulse imperfections is illustrated in figure 2*a*. The experimental data points represent the survival probability of the three Cartesian components of the system qubit. Like all experimental data in this paper, these measurements were performed on the ^{13}C nuclear spins of polycrystalline adamantane, using a home-built NMR spectrometer with a ^{1}H resonance frequency of 300 MHz. The duration of the π-pulses was $\approx 10\,\mu$s. In this system, the dephasing of the nuclear spins originates from the interaction with an environment consisting of ^{1}H nuclear spins and can be considered as a pure dephasing process. The first sequence considered in the figure is CPMG. In this case, the decay of the magnetization is very slow when the system is initially oriented parallel to the rotation axis of the pulse (longitudinal state). As we discuss later, this is an indication that the pulse errors have no effect on this initial state. In contrast, for the transverse initial states, the errors of the individual pulses accumulate and lead to a rapid decay. A similar behaviour is found for the UDD sequence, which also uses rotations around a single axis [55,65].

The second DD sequence considered in figure 2 is the XY-4 sequence, which consists of pulses applied along the x- and y-axes. The alternating phases of the pulses result in a partial cancellation of pulse errors, independent of the initial condition [35,36]. As a result, the performance of this sequence is much more symmetric with respect to the initial state in the xy-plane and the average decay times are significantly longer [54,55].

In the context of QIP, it is important that the performance of gate operations be independent of the initial conditions (which typically are unknown). A common choice for quantifying the performance of a general quantum operation is then the fidelity F [99]:

$$F = \frac{|\mathrm{Tr}(AB^{\dagger})|}{\sqrt{\mathrm{Tr}(AA^{\dagger})\mathrm{Tr}(BB^{\dagger})}}. \tag{3.1}$$

Here, A is the target propagator for the process and B the actual propagator. For the present situation, where the goal is a quantum memory, the target propagator is the identity operation I.

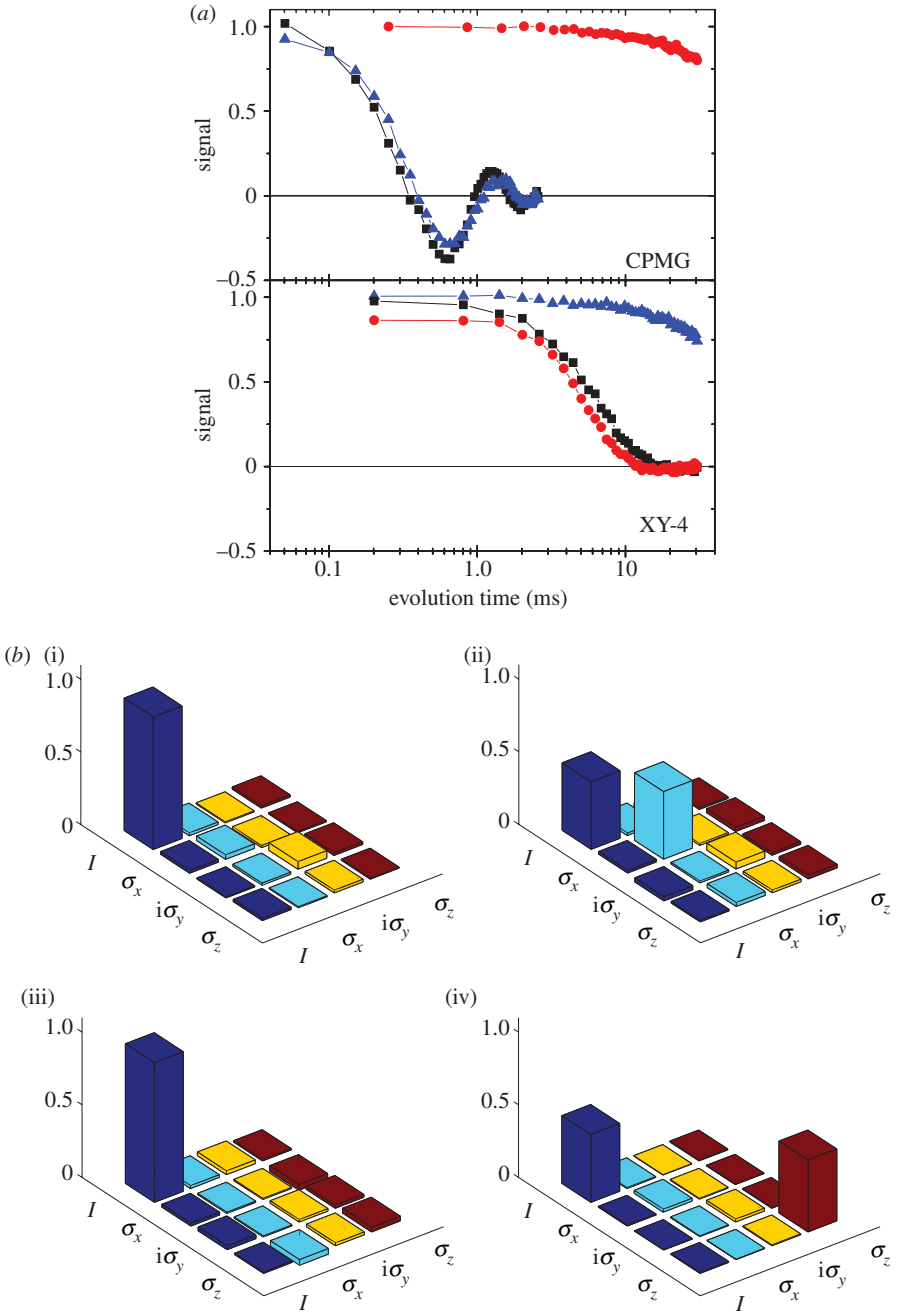

Figure 2. Comparison between two basic DD sequences: CPMG, which is not robust against errors, and the self-correcting sequence XY-4. (*a*) Normalized magnetization as a function of time (circles, x; squares, y; triangles, z). The delay $\tau = 40\,\mu s$ between the pulses is constant and identical for both sequences. (*b*) The real part of the process matrices χ for CPMG ((i) 1 cycle, (ii) 40 cycles) and XY-4 ((iii) 1 cycle, (iv) 40 cycles). Here, the cycle times are $\tau_c = 85\,\mu s$ for CPMG and $\tau_c = 170\,\mu s$ for XY-4. The imaginary part, which is very small, is not shown. (Online version in colour.)

The actual propagators are not always unitary. We therefore write the process as

$$\rho_{\mathrm{f}} = \sum_{nm} \chi_{mn} E_m \rho_{\mathrm{i}} E_n^{\dagger}, \tag{3.2}$$

where ρ_{i} and ρ_{f} are the density matrices at the beginning and end of the process. The operators E_m must form a basis. For the present case, we choose them as $E_m = (I, \sigma_x, i\sigma_y, \sigma_z)$. The ideal and actual processes can therefore be quantified by the matrix elements χ_{mn}. For the target evolution, the χ-matrix is

$$\chi_I = \begin{pmatrix} 1 & 0 & 0 & 0 \\ 0 & 0 & 0 & 0 \\ 0 & 0 & 0 & 0 \\ 0 & 0 & 0 & 0 \end{pmatrix}. \tag{3.3}$$

The matrix elements for the actual process are determined experimentally by quantum process tomography [3,100]. We use them to calculate the process fidelity from equation (3.1). In figure 2*b*, we compare the real part of the experimental χ matrices for the two sequences. After one cycle, the process matrices for both sequences represent an evolution that is close to the identity operation. The fidelity between the experimental matrices and the ideal matrix (3.3) is 0.988 and 0.989 for the CPMG and XY-4 cycles, respectively. Measured over 40 cycles, the process matrices of the two sequences differ significantly from the identity operation, but also from each other. For the XY-4 sequence, the non-vanishing elements are $\chi_{11} = 0.46$ and $\chi_{44} = 0.51$, while for CPMG the non-vanishing elements are $\chi_{11} = 0.46$ and $\chi_{22} = 0.47$. The two matrices represent therefore qualitatively different processes. Under the XY-4 sequence, the transverse components x and y decay more rapidly and the system evolves towards an intermediate state

$$\rho_{\mathrm{f}} = 0.5(\rho_{\mathrm{i}} + \sigma_z \rho_{\mathrm{i}} \sigma_z). \tag{3.4}$$

If we write the initial state as

$$\rho_{\mathrm{i}} = x\sigma_x + y\sigma_y + z\sigma_z,$$

the final state becomes

$$\rho_{\mathrm{f}} = 0.5(x\sigma_x + y\sigma_y + z\sigma_z) + 0.5(-x\sigma_x - y\sigma_y + z\sigma_z) = z\sigma_z. \tag{3.5}$$

This corresponds to a projection of the density operator onto the z-axis, i.e. to a complete dephasing of the transverse components in the xy-plane. The longer lifetime of the z-component is a consequence of the fact that it does not commute with the SE coupling and therefore is not affected by dephasing.

The CPMG sequence, conversely, projects the density operator after many cycles onto the x-axis:

$$\rho_{\mathrm{f}} = 0.5\rho_{\mathrm{i}} + 0.5\sigma_x \rho_{\mathrm{i}} \sigma_x = x\sigma_x. \tag{3.6}$$

The CPMG is a spin-lock sequence [101] that retains the magnetization along the x direction but destroys the components perpendicular to it. Because a real experimental implementation always generates a distribution of control field

amplitudes, spins at different positions precess with different rates around the direction of the radio-frequency field. As a result, the perpendicular components become completely randomized after a sufficiently large overall flip angle as shown in figure 2*a*.

While these examples demonstrate the effect of pulse imperfections, the next section shows different strategies for making decoupling sequences robust against such errors.

4. Robust decoupling sequences

We have to make decoupling insensitive to pulse imperfections. Different possibilities for generating high-fidelity sequences have been proposed in the context of QIP [46,54,81]. Here, we discuss two possible approaches: first, we show that it is possible to replace individual refocusing pulses by compensated pulses that implement very precise inversions, and then we discuss sequences that are inherently robust, i.e. insensitive to the imperfections of the individual pulses.

(*a*) *Robust pulses*

The simplest approach to make a sequence robust consists of replacing every refocusing pulse by a robust composite pulse [102]. The composite pulses are sequences of consecutive pulses designed to be robust against various classes of imperfections. They generate rotations that are close to the ideal rotation even in the presence of errors. Particularly useful for quantum information applications are those composite pulses that produce compensated rotations for any initial condition, denominated in the NMR literature as class-A pulses [102].

Recent experiments have successfully used composite pulses to demonstrate the resulting increase of the performance of different DD sequences [54,56]. These works have implemented the composite pulse defined as

$$(\pi)_{\pi/6+\phi} - (\pi)_{\phi} - (\pi)_{\pi/2+\phi} - (\pi)_{\phi} - (\pi)_{\pi/6+\phi}, \tag{4.1}$$

which is equivalent to a robust π rotation around the axis defined by ϕ followed by a $-\pi/3$ rotation around the z-axis [103]. For cyclic sequences, which always consist of even numbers of π rotations, the effect of the additional z rotation vanishes if the flip angle errors are sufficiently small.

A comparison between standard sequences (not using robust pulses) against sequences with robust pulses has been reported [54]. It was observed that robust pulses improve the performance at high duty cycles. However, for low duty cycles, standard sequences perform better for the same duty cycle, because the pulse spacing is shorter in that case. Thus, if the objective is only to preserve a quantum state, the best performance is obtained at high duty cycles, using robust pulses. The best sequences that are suitable for parallel application of quantum gate operations are the self-correcting sequences discussed later.

The composite pulses are usually designed to correct flip angle errors and offset errors. For compensating the effects introduced by the finite length of pulses, some theoretical works have proposed that a finite pulse could be approximated as an instantaneous one by using an appropriate shaped pulse [104–106]. Such shaped pulses can significantly improve the performance of the decoupling sequences.

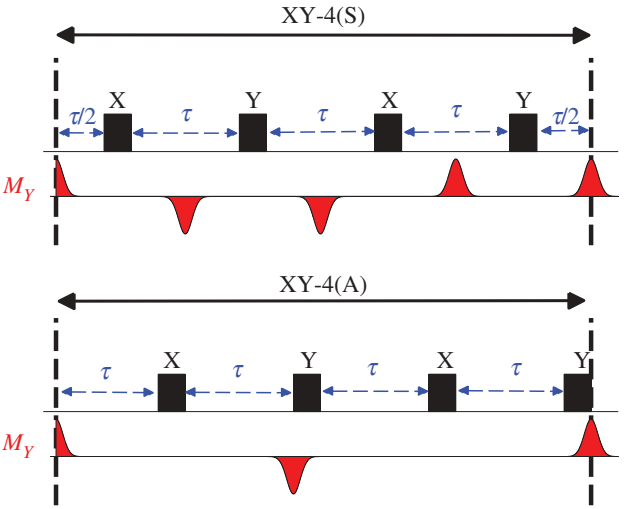

Figure 3. Schematic of time symmetric XY-4(S) and asymmetric XY-4(A). (Online version in colour.)

(*b*) *Self-correcting sequences*

An alternative to the use of composite pulses consists of making the decoupling sequences fault-tolerant without compensating the error of each pulse, but by designing them in such a way that the error introduced by one pulse is compensated by the other pulses of the cycle [54]. A straightforward strategy for designing improved sequences consists of sequentially combining variants of a basic cycle to longer and more robust cycles.

Being the shortest universal decoupling cycle, the XY-4 cycle is often chosen as the basic building block for constructing higher order compensated sequences. In the spectroscopy and quantum computing communities, two versions of the XY-4 sequence are used [67]. The basic cycle originally introduced in NMR shows reflection symmetry with respect to the centre of the cycle. In contrast to that, the sequence used in the quantum information community is time-asymmetric. One consequence of this small difference is that in the symmetric version, the echoes are formed in the centre of the windows between any two pulses, while in the case of asymmetric cycles, the echoes coincide with every second pulse, as shown in figure 3. The separation in time between the echoes is therefore twice as long in this case. If the environment is not static, the larger separation of the echoes leads to a faster decay of the echo amplitude [67].

If a robust pulse contains only π rotations, as in the case of (4.1), it is also possible to convert such a composite pulse into a decoupling cycle by inserting delays between the individual π rotations. This approach has been used [54] to build a self-correcting sequence. The building block is

$$\begin{aligned}\mathrm{KDD}_\phi = {} & f_{\tau/2} - (\pi)_{\pi/6+\phi} - f_\tau - (\pi)_\phi - f_\tau - (\pi)_{\pi/2+\phi} - f_\tau - (\pi)_\phi \\ & - f_\tau - (\pi)_{\pi/6+\phi} - f_{\tau/2}. \end{aligned} \tag{4.2}$$

The self-correcting sequence is created by combining two such 5-pulse blocks shifted in phase by $\pi/2$ to $[\mathrm{KDD}_\phi\text{–}\mathrm{KDD}_{\phi+\pi/2}]^2$, where the lower index gives the

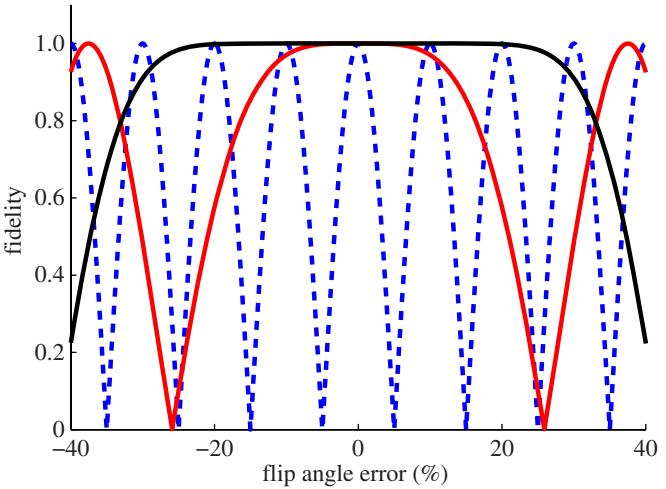

Figure 4. Simulation of fidelity as a function of the flip angle error for KDD (black solid line), XY-4 (grey solid line) and CPMG (grey dashed line) cycles. The fidelity was calculated from equation (3.1) by choosing the identity as the target operator A and calculating the actual propagator B from the pulse sequence with different flip angle errors. (Online version in colour.)

overall phase of the block and $[.]^2$ indicates that the full cycle, which implements a unit propagator, consists of a total of 20 π pulses. We refer to this as the KDD sequence [54].

In figure 4, we show how strongly errors in the flip angles of individual pulses affect the fidelity of the pulse sequence. Neglecting the effect of the environment, we calculate the fidelity F after the application of 20 pulses to a single spin as a function of the flip angle error. The figure compares the fidelities for the CPMG, XY-4 and KDD cycles. For the CPMG sequence, the fidelity drops to less than 95 per cent if the flip angle error exceeds $\approx 2\%$. For the XY-4 sequence, this bandwidth increases to $\approx 10\%$ and for KDD to $\approx 30\%$. KDD and XY-4 are obviously much less susceptible to pulse imperfections than CPMG. The low fidelities observed for CPMG are experimentally manifested by the fast decay of the transverse components, such as M_x in figure 2.

(*c*) *Combining basic cycles*

Every decoupling sequence contains unwanted terms in the average Hamiltonian. They can be reduced by combining different versions of the basic cycles in such a way that some of the error terms cancel. Two different versions of this procedure have been used: the basic cycles can be applied subsequently [36] or one cycle can be inserted into the delays of another cycle [46,81]. The first approach was introduced in NMR, e.g. for designing high-performance homonuclear decoupling sequences [38–43] or in high-resolution heteronuclear decoupling [31–33,35–37]. Examples of DD sequences that can be constructed using this approach are the XY-8 and XY-16 sequences [36]. The XY-8 is created by combining a XY-4 cycle with its time-reversed image, while XY-16 is created by combining the XY-8 with its phase-shifted copy.

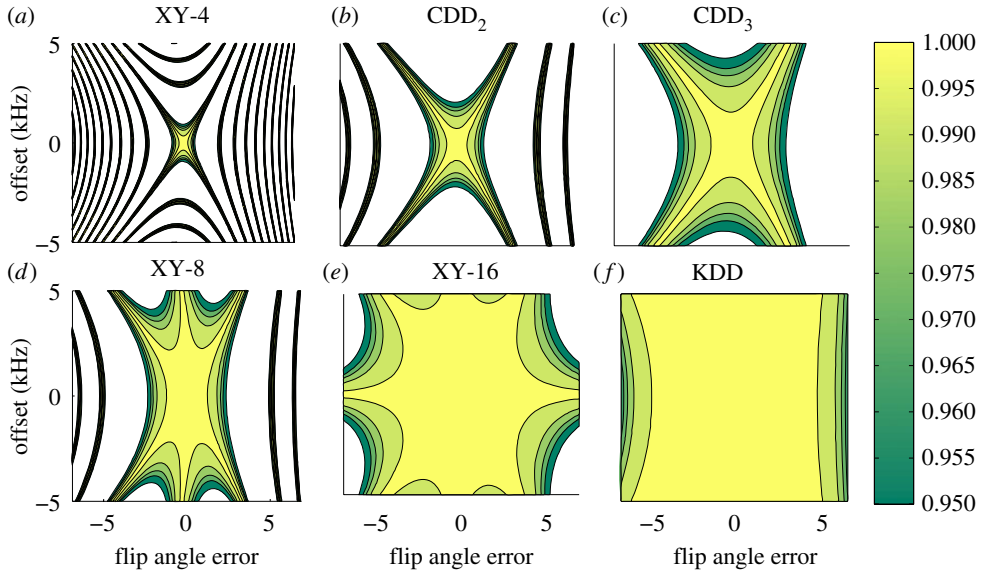

Figure 5. Error tolerance of different self-correcting sequences. The upper row (a–c) shows the calculated fidelity F for CDD sequences, while the lower row (d–f) shows the results for the XY-8, XY-16 and KDD sequences. Each panel shows the fidelity after 1680 pulses as a function of flip-angle error and offset error. The regions where the fidelity is lower than 0.95 are shown in white. The fidelity was calculated from equation (3.1) by choosing the identity as the target operator A and calculating the actual propagator B from the pulse sequence with different flip angle and offset errors. (Online version in colour.)

The second approach is the concatenation scheme proposed by Khodjasteh & Lidar [46,81]. It generates the CDD sequence of order $N+1$ by inserting CDD_N cycles into the delays of the XY-4 sequence (figure 1). Ideally, each level of concatenation improves the decoupling performance and the tolerance to pulse imperfections; in practice, higher order sequences do not always perform better. It has been theoretically predicted [45,81,82] and later observed experimentally that the finite duration of the pulses and constrained delays between pulses result in the existence of optimal levels of concatenation [54,55].

In figure 5, we demonstrate how the well-designed combination of basic cycles can lead to extended cycles with better error compensation. Here, we consider as the leading experimental imperfections deviations of the amplitude and frequency of each pulse. Neglecting the effect of the environment, we calculate the fidelity F after applying 1680 pulses to the system as a function of the two error parameters. Each panel contains the colour-coded fidelity for one of six different decoupling sequences. The yellow area inside the highest contour line corresponds to fidelities greater than 99 per cent, which is the best threshold known for reliable quantum computing. In figure 5a–c, the increasing size of this yellow area demonstrates the improvement in error tolerance due to the CDD scheme of concatenation. Figure 5a,d,e shows the same result for the sequential concatenation scheme, where only two cycles are combined at each step: concatenation of the XY-4 cycle with its time-inverted and phase-shifted copies forms the XY-8 and XY-16

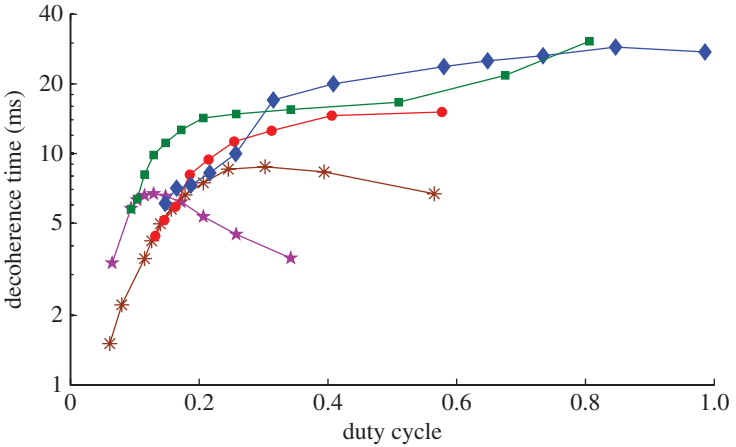

Figure 6. Experimental decoherence times for different compensated DD sequences as a function of the duty cycle. The qubits used for this experiment were ^{13}C nuclear spins in a polycrystalline adamantane sample [54,55,65,67]. Stars, XY-4 = CDD_1; asterisks, CDD_2; circles, CDD_3; diamonds, CDD_4; squares, KDD. (Online version in colour.)

sequences. The 16-pulse XY-16 cycle is significantly more robust than the 84-pulse CDD_3 cycle. The best performance is achieved by the KDD sequence, whose cycle consists of 20 pulses.

In figure 6, we compare the experimental performance of different self-correcting sequences. For the low-order sequences XY-4 and CDD_2, the decoherence time reaches a maximum with increasing duty cycle (= decreasing pulse spacing), indicating that for higher duty cycles the pulse errors dominate. Higher order CDD sequences, in particular CDD_4, appear to be much more efficient in compensating these pulse errors, as evidenced by long decoherence times at high duty cycles. However, these sequences show lower performance at low duty cycles, which may be associated with the fact that the duration of these cycles exceeds the bath correlation time if the duty cycle is reduced. The KDD sequence, which has a significantly shorter cycle time, but still excellent compensation, yields the longest decoherence times over the full range of duty cycles. It appears therefore to be useful for both quantum computing and state preservation.

(*d*) *Time reversal symmetry*

The symmetry of the basic building blocks plays a key role in determining the performance of the concatenated higher order sequences. Two sequences constructed according to the same rules from a basic block have different propagators if the basic blocks are symmetric or not [54,67]. For example, if we concatenate four XY-4 cycles to the XY-16 sequence, we obtain new cycles, which are time-symmetric, independent of which version of the XY-4 sequence was used for the building blocks. Although all the odd order terms vanish in the average Hamiltonians of both versions, the even order terms of the sequences that are built from asymmetric blocks contain additional unwanted terms [67].

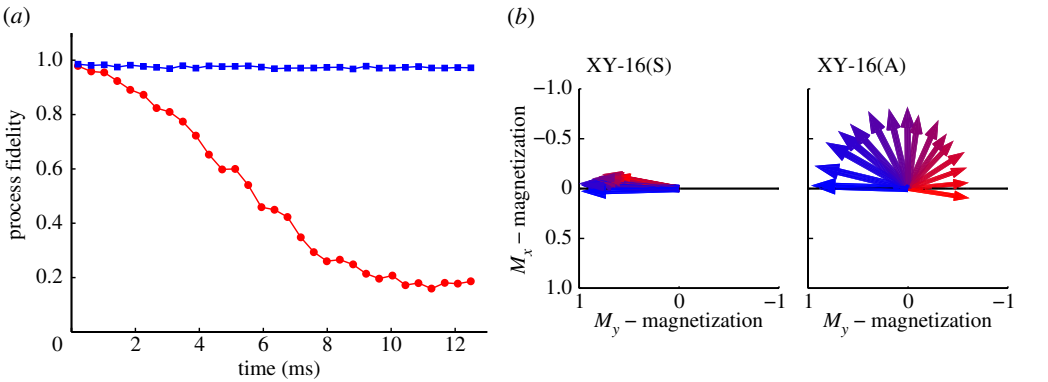

Figure 7. Comparison between the two forms of the XY-16 sequence: XY-16(S), built from the symmetric version of the XY-4 cycle, and XY-16(A), built from the asymmetric block. The delay $\tau = 10\,\mu s$ between the pulses is constant and identical for both sequences. (*a*) The process fidelity as a function of time (blue squares, XY-16(S); red circles, XY-16(A)). (*b*) The Bloch vector in the *xy* plane at different times. The colour code in (*b*) denotes the time evolution, blue for the initial state and red for the final state. The qubits used for this experiment were ^{13}C nuclear spins in a polycrystalline adamantane sample [54,55,65,67]. (Online version in colour.)

The different behaviour of sequences consisting of symmetric versus asymmetric blocks is illustrated in figure 7. If we start from the symmetric form of XY-4, the resulting XY-16 sequence shows much better performance than the sequence using the asymmetric XY-4 as the building block. Analogous results were obtained for the two versions of the XY-8 sequence [67].

Earlier experiments showed two different contributions to the overall fidelity loss [67]: a precession around the *z*-axis (which can be attributed to the combined effect of flip-angle errors) and an overall reduction of the amplitude (which results from the SE interaction). The combination of precession and reduction of amplitude is illustrated in figure 7*b*. It shows the *xy*-components of the magnetization at different times during the XY-16 sequence. If the XY-16 sequence is built by the asymmetric form of XY-4, a distinct precession around the *z*-axis is observed. This causes a deviation from the desired evolution and reduces therefore the fidelity of the process. However, for the sequence consisting of symmetric blocks, the precession is negligible. These results suggest that pulse errors are better compensated by concatenating symmetric building blocks.

The same concept can also be applied to CDD sequences. The conventional concatenation scheme of equation (2.6) uses asymmetric building blocks and is not compatible with the symmetric version of XY-4. A new concatenation scheme was therefore proposed in [54,67]. In this scheme, the symmetrized version of CDD is constructed as

$$\mathrm{CDD}_{N+1} = [\sqrt{\mathrm{CDD}_N} - X - \mathrm{CDD}_N - Y - \sqrt{\mathrm{CDD}_N}]^2. \tag{4.3}$$

In figure 8, we compare the process fidelities for the two versions of the CDD_2 sequence. As in the XY sequences, clearly, the symmetrized version, CDD_2(S), shows a significantly improved performance, compared with the standard CDD_2(A) version. In [67], it was experimentally observed that the

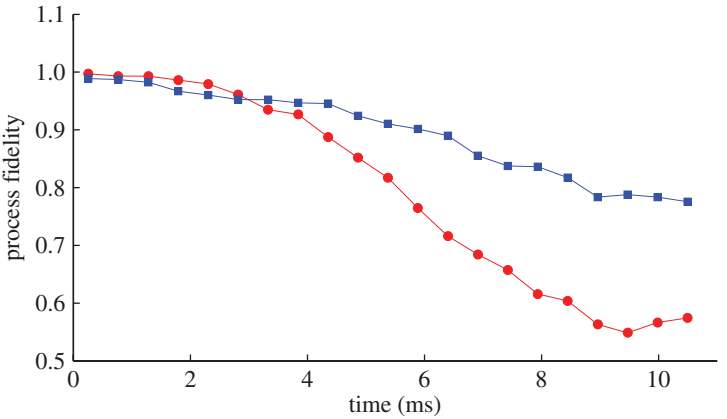

Figure 8. Experimental fidelity decay for $CDD_2(S)$ (squares) and $CDD_2(A)$ (circles) built from symmetric and asymmetric blocks. The delay $\tau = 10\,\mu s$ between the pulses is constant and identical for both sequences. The qubits used for this experiment were ^{13}C nuclear spins in a polycrystalline adamantane sample [54,55,65,67]. (Online version in colour.)

performance of all DD sequences based on symmetric building blocks is better than or equal to that of sequences using non-symmetric building blocks. This behaviour is consistent with general arguments based on average Hamiltonian theory [107,108].

5. Conclusion and perspectives

DD is becoming a standard technique for preserving the coherence of quantum mechanical systems, which does not need control over the environmental degrees of freedom. The technique aims to reduce decoherence rates by attenuating the SE interaction with a periodic sequence of π pulses applied to the qubits. The pioneering strategies for decoupling were introduced in the context of NMR spectroscopy [31]. Since then, many different decoupling sequences have been developed in the context of NMR [32,33,35,36] or QIP [44,46,47,50,53,54,81,97,98].

Generally, we can divide the DD sequences in two groups: (i) sequences that involve pulses with identical rotation axes and (ii) sequences that contain pulses in different directions. The type (i) sequences are strongly sensitive to pulse errors and are only capable of suppressing the effects of a purely dephasing environment or pure spin–flip interactions. Examples of such DD sequences are CPMG and UDD. The second group can suppress a general SE interaction and usually exhibits better tolerance to experimental imperfections. Examples of such sequences are the XY family (XY-4, XY-8 and XY-16), the CDD sequences and the KDD sequence.

Recent experiments have successfully implemented DD methods and demonstrated the resulting increase of the coherence times by several orders of magnitude [54–56,67]. These works also showed that the main limitation to the reduction of the decay rates is the imperfections of the pulse. Two approaches

have been used to correct this. The first approach replaces the inversion pulses by robust composite pulses [102], which generate rotations that are close to the target value even in the presence of pulse errors. In this case, the pulses are corrected individually. The second approach consists of designing the decoupling sequences in such a way that the error introduced by one pulse is compensated by the other pulses, without compensating the error of each pulse individually. The properties of basic decoupling cycles can be further improved by concatenating basic cycles into longer and more robust cycles. The concatenation can be made either by combining symmetry-related copies of a basic cycle subsequently [36] (resulting in the XY-8 and XY-16 sequences) or by inserting the basic cycle into the delays of another cycle [46,81] (CDD sequences).

The time reversal symmetry of the basic building blocks is a useful criterion for minimizing error contributions. It has been demonstrated that the sequences built from symmetric building blocks often perform better and never worse than sequences built from non-symmetric blocks [54,67]. This is a significant advantage, considering that the complexities of the sequences based on symmetric or asymmetric blocks are identical.

Earlier experiments [54] showed that the best sequences that are suitable for parallel application of quantum gate operations are the symmetric self-correcting sequences. However, as the delay between pulses decreases, sequences with robust pulses perform better. Thus, if the objective is only to preserve a quantum state, the best performance is achieved by using robust pulses to correct pulse errors. On the other hand, the KDD sequence introduced in Souza *et al.* [54] combines the useful properties of self-correcting sequences with those of robust pulses and can thus be used for both quantum memory and quantum computing.

During the last few years, many advances have been achieved. However, for the application of the technique in real quantum devices, further studies will certainly be required. So far, most work has focused on single qubit systems. In the future, more experimental tests will be needed with multi-qubit systems. In the field of quantum computation, another important development may result from the combination of DD sequences with those techniques used to implement robust quantum gates [28,30,109,110]. DD does not require auxiliary qubits or measurements, and it may be helpful for reaching the error threshold for reliable quantum computation. Some theoretical works [76–79] proposed methods for combining DD with quantum error correction. Future research on DD will also consider applications outside QIP. Recent experiments have applied DD pulse sequences, for example, to probe the noise spectrum directly [69–71] and detect weak magnetic fields [72–75].

We acknowledge useful discussions with Daniel Lidar and Gregory Quiroz. This work is supported by the DFG through Su 192/24-1.

References

1 Shor, P. W. 1996 Polynomial-time algorithms for prime factorization and discrete logarithms on a quantum compute. *SIAM J. Comput.* **26**, 1484–1509. (doi:10.1137/S0097539795293172)

2 DiVincenzo, D. P. 1995 Quantum computation. *Science* **270**, 255–261. (doi:10.1126/science.270.5234.255)

3 Nielsen, M. A. & Chuang, I. L. 2000 *Quantum computation and quantum information.* Cambridge, UK: Cambridge University Press.

4 Bennett, C. H. & DiVincenzo, D. P. 2000 Quantum information and computation. *Nature* **404**, 247–255. (doi:10.1038/35005001)

5 Zurek, W. H. 2003 Decoherence, einselection, and the quantum origins of the classical. *Rev. Mod. Phys.* **75**, 715–775. (doi:10.1103/RevModPhys.75.715)

6 Krojanski, H. G. & Suter, D. 2004 Scaling of decoherence in wide NMR quantum registers. *Phys. Rev. Lett.* **93**, 090501. (doi:10.1103/PhysRevLett.93.090501)

7 Krojanski, H. G. & Suter, D. 2006 Reduced decoherence in large quantum registers. *Phys. Rev. Lett.* **97**, 150503. (doi:10.1103/PhysRevLett.97.150503)

8 Krojanski, H. G. & Suter, D. 2006 Decoherence in large NMR quantum registers. *Phys. Rev. A* **74**, 062319. (doi:10.1103/PhysRevA.74.062319)

9 Cho, H., Cappellaro, P., Cory, D. G. & Ramanathan, C. 2006 Decay of highly correlated spin states in a dipolar-coupled solid: NMR study of CaF_2. *Phys. Rev. B* **74**, 224434. (doi:10.1103/PhysRevB.74.224434)

10 Lovric, M., Krojanski, H. & Suter, D. 2007 Decoherence in large quantum registers under variable interaction with the environment. *Phys. Rev. A* **75**, 042305. (doi:10.1103/PhysRevA.75.042305)

11 Sánchez, C. M., Pastawski, H. M. & Levstein, P. R. 2007 Time evolution of multiple quantum coherences in NMR. *Physica B* **398**, 472–475. (doi:10.1016/j.physb.2007.04.092)

12 Doronin, S. I., Fel'dman, E. B. & Zenchuk, A. I. 2011 Numerical analysis of relaxation times of multiple quantum coherences in the system with a large number of spins. *J. Chem. Phys.* **134**, 034102. (doi:10.1063/1.3528040)

13 Zobov, V. E. & Lundin, A. A. 2011 Decay of multispin multiquantum coherent states in the NMR of a solid. *J. Exp. Theor. Phys.* **112**, 451–459. (doi:10.1134/S1063776111020129)

14 Rhim, W. K., Pines, A. & Waugh, J. S. 1970 Violation of the spin temperature hypothesis. *Phys. Rev. Lett.* **25**, 218–220. (doi:10.1103/PhysRevLett.25.218)

15 Zhang, S., Meier, B. H. & Ernst, R. R. 1992 Polarization echoes in NMR. *Phys. Rev. Lett.* **69**, 2149–2151. (doi:10.1103/PhysRevLett.69.2149)

16 Usaj, H. P. G. & Levstein, P. 1998 Gaussian to exponential crossover in the attenuation of polarization echoes in NMR. *Mol. Phys.* **95**, 1229–1236. (doi:10.1080/00268979809483253)

17 Pastawski, H. M., Levstein, P. R., Usaj, G., Raya, J. & Hirschinger, J. A. 2000 A nuclear magnetic resonance answer to the Boltzmann–Loschmidt controversy? *Physica A* **283**, 166–170. (doi:10.1016/S0378-4371(00)00146-1)

18 Jalabert, R. A. & Pastawski, H. M. 2001 Environment-independent decoherence rate in classically chaotic systems. *Phys. Rev. Lett.* **86**, 2490–2493. (doi:10.1103/PhysRevLett.86.2490)

19 Álvarez, G. A. & Suter, D. 2010 NMR quantum simulation of localization effects induced by decoherence. *Phys. Rev. Lett.* **104**, 230403. (doi:10.1103/PhysRevLett.104.230403)

20 Álvarez, G. A. & Suter, D. 2011 Localization effects induced by decoherence in superpositions of many-spin quantum states. *Phys. Rev. A* **84**, 012320. (doi:10.1103/PhysRevA.84.012320)

21 Anderson, P. 1958 Absence of diffusion in certain random lattices. *Phys. Rev.* **109**, 1492–1505. (doi:10.1103/PhysRev.109.1492)

22 Pomeransky, A. & Shepelyansky, D. 2004 Quantum computation of the Anderson transition in the presence of imperfections. *Phys. Rev. A* **69**, 014302. (doi:10.1103/PhysRevA.69.014302)

23 Chiara, G. D., Rossini, D., Montangero, S. & Fazio, R. 2005 From perfect to fractal transmission in spin chains. *Phys. Rev. A* **72**, 012323. (doi:10.1103/PhysRevA.72.012323)

24 Burrell, C. K. & Osborne, T. J. 2007 Bounds on the speed of information propagation in disordered quantum spin chains. *Phys. Rev. Lett.* **99**, 167201. (doi:10.1103/PhysRevLett.99.167201)

25 Keating, J., Linden, N., Matthews, J. & Winter, A. 2007 Localization and its consequences for quantum walk algorithms and quantum communication. *Phys. Rev. A* **76**, 012315. (doi:10.1103/PhysRevA.76.012315)

26 Apollaro, T. & Plastina, F. 2007 Quantum information storage in the localized state of a spin chain. *Open Syst. Inform. Dyn.* **14**, 41–51. (doi:10.1007/s11080-007-9027-5)

27 Allcock, J. & Linden, N. 2009 Quantum communication beyond the localization length in disordered spin chains. *Phys. Rev. Lett.* **102**, 110501. (doi:10.1103/PhysRevLett.102.110501)

28 Knill, E., Laflamme, R. & Zurek, W. H. 1998 Resilient quantum computation. *Science* **279**, 342–345. (doi:10.1126/science.279.5349.342)
29 Preskill, J. 1998 Reliable quantum computers. *Proc. R. Soc. Lond. A* **454**, 385–410. (doi:10.1098/rspa.1998.0167)
30 Knill, E. 2005 Quantum computing with realistically noisy devices. *Nature* **434**, 39–44. (doi:10.1038/nature03350)
31 Hahn, E. L. 1950 Spin echoes. *Phys. Rev.* **80**, 580–594. (doi:10.1103/PhysRev.80.580)
32 Carr, H. Y. & Purcell, E. M. 1954 Effects of diffusion on free precession in nuclear magnetic resonance experiments. *Phys. Rev.* **94**, 630–638. (doi:10.1103/PhysRev.94.630)
33 Meiboom, S. & Gill, D. 1958 Modified spin-echo method for measuring nuclear relaxation times. *Rev. Sci. Instrum.* **29**, 688–691. (doi:10.1063/1.1716296)
34 Waugh, J. S., Wang, C. H., Huber, L. M. & Vold, R. L. 1968 Multiple-pulse NMR experiments. *J. Chem. Phys.* **48**, 662–670. (doi:10.1063/1.1668698)
35 Maudsley, A. A. 1986 Modified Carr–Purcell–Meiboom–Gill sequence for NMR fourier imaging applications. *J. Magn. Reson.* **69**, 488–491. (doi:10.1016/0022-2364(86)90160-5)
36 Gullion, T., Baker, D. B. & Conradi, M. S. 1990 New, compensated Carr-Purcell sequences. *J. Magn. Reson.* **89**, 479–484. (doi:10.1016/0022-2364(90)90331-3)
37 Waugh, J. S. 1982 Theory of broadband spin decoupling. *J. Magn. Reson.* **50**, 30–49. (doi:10.1016/0022-2364(82)90029-4)
38 Waugh, J. S., Huber, L. M. & Haeberlen, U. 1968 Approach to high-resolution NMR in solids. *Phys. Rev. Lett.* **20**, 180–182. (doi:10.1103/PhysRevLett.20.180)
39 Mansfield, P., Orchard, M. J., Stalker, D. C. & Richards, K. H. B. 1973 Symmetrized multipulse nuclear-magnetic-resonance experiments in solids: measurement of the chemical-shift shielding tensor in some compounds. *Phys. Rev. B* **7**, 90–105. (doi:10.1103/PhysRevB.7.90)
40 Rhim, W. K., Elleman, D. D. & Vaughan, R. W. 1973 Analysis of multiple pulse NMR in solids. *J. Chem. Phys.* **59**, 3740–3749. (doi:10.1063/1.1680545)
41 Rhim, W. K., Elleman, D. D., Schreiber, L. B. & Vaughan, R. W. 1974 Analysis of multiple pulse NMR in solids. II. *J. Chem. Phys.* **60**, 4595–4604. (doi:10.1063/1.1680944)
42 Burum, D. P. & Rhim, W. K. 1979 Analysis of multiple pulse NMR in solids. III. *J. Chem. Phys.* **71**, 944–956. (doi:10.1063/1.438385)
43 Burum, D. P., Linden, M. & Ernst, R. R. 1981 Low-power multipulse line narrowing in solid-state NMR. *J. Magn. Reson.* **44**, 173–188. (doi:10.1016/0022-2364(81)90200-6)
44 Viola, L., Knill, E. & Lloyd, S. 1999 Dynamical decoupling of open quantum systems. *Phys. Rev. Lett.* **82**, 2417–2421. (doi:10.1103/PhysRevLett.82.2417)
45 Viola, L. & Knill, E. 2003 Robust dynamical decoupling of quantum systems with bounded controls. *Phys. Rev. Lett.* **90**, 037901. (doi:10.1103/PhysRevLett.90.037901)
46 Khodjasteh, K. & Lidar, D. A. 2005 Fault-tolerant quantum dynamical decoupling. *Phys. Rev. Lett.* **95**, 180501. (doi:10.1103/PhysRevLett.95.180501)
47 Uhrig, G. S. 2007 Keeping a quantum bit alive by optimized π-pulse sequences. *Phys. Rev. Lett.* **98**, 100504. (doi:10.1103/PhysRevLett.98.100504)
48 Gordon, G., Kurizki, G. & Lidar, D. A. 2008 Optimal dynamical decoherence control of a qubit. *Phys. Rev. Lett.* **101**, 010403. (doi:10.1103/PhysRevLett.101.010403)
49 Biercuk, M. J., Uys, H., VanDevender, A. P., Shiga, N., Itano, W. M. & Bollinger, J. J. 2009 Optimized dynamical decoupling in a model quantum memory. *Nature* **458**, 996–1000. (doi:10.1038/nature07951)
50 Uhrig, G. S. 2009 Concatenated control sequences based on optimized dynamic decoupling. *Phys. Rev. Lett.* **102**, 120502. (doi:10.1103/PhysRevLett.102.120502)
51 Yang, W., Wang, Z. & Liu, R. 2010 Preserving qubit coherence by dynamical decoupling. *Front. Phys.* **6**, 2–14. (doi:10.1007/s11467-010-0113-8)
52 Clausen, J., Bensky, G. & Kurizki, G. 2010 Bath-optimized minimal-energy protection of quantum operations from decoherence. *Phys. Rev. Lett.* **104**, 040401. (doi:10.1103/PhysRevLett.104.040401)
53 West, J. R., Fong, B. H. & Lidar, D. A. 2010 Near-optimal dynamical decoupling of a qubit. *Phys. Rev. Lett.* **104**, 130501. (doi:10.1103/PhysRevLett.104.130501)

54 Souza, A. M., Álvarez, G. A. & Suter, D. 2011 Robust dynamical decoupling for quantum computing and quantum memory. *Phys. Rev. Lett.* **106**, 240501. (doi:10.1103/PhysRevLett.106.240501)

55 Álvarez, G. A., Ajoy, A., Peng, X. & Suter, D. 2010 Performance comparison of dynamical decoupling sequences for a qubit in a rapidly fluctuating spin bath. *Phys. Rev. A* **82**, 042306. (doi:10.1103/PhysRevA.82.042306)

56 Ryan, C. A., Hodges, J. S. & Cory, D. G. 2010 Robust decoupling techniques to extend quantum coherence in diamond. *Phys. Rev. Lett.* **105**, 200402. (doi:10.1103/PhysRevLett.105.200402)

57 Wang, Z. & Dobrovitski, V. V. 2011 Aperiodic dynamical decoupling sequences in the presence of pulse errors. *J. Phys. B* **44**, 154004. (doi:10.1088/0953-4075/44/15/154004)

58 Xiao, Z., He, L. & Wang, W. 2011 Efficiency of dynamical decoupling sequences in the presence of pulse errors. *Phys. Rev. A* **83**, 032322. (doi:10.1103/PhysRevA.83.032322)

59 Morton, J. J. L., Tyryshkin, A. M., Ardavan, A., Benjamin, S. C., Porfyrakis, K., Lyon, S. A. & Briggs, G. A. D. 2006 Bang-bang control of fullerene qubits using ultra-fast phase gates. *Nat. Phys.* **2**, 40–43. (doi:10.1038/nphys192)

60 Morton, J. J. L. *et al.* 2008 Solid-state quantum memory using the ^{31}P nuclear spin. *Nature* **455**, 1085–1088. (doi:10.1038/nature07295)

61 Du, J., Rong, X., Zhao, N., Wang, Y., Yang, J. & Liu, R. B. 2009 Preserving electron spin coherence in solids by optimal dynamical decoupling. *Nature* **461**, 1265–1268. (doi:10.1038/nature08470)

62 de Lange, G., Wang, Z. H., Riste, D., Dobrovitski, V. V. & Hanson, R. 2010 Universal dynamical decoupling of a single solid-state spin from a spin bath. *Science* **330**, 60–63. (doi:10.1126/science.1192739)

63 Barthel, C., Medford, J., Marcus, C. M., Hanson, M. P. & Gossard, A. C. 2010 Interlaced dynamical decoupling and coherent operation of a singlet–triplet qubit. *Phys. Rev. Lett.* **105**, 266808. (doi:10.1103/PhysRevLett.105.266808)

64 Bluhm, H., Foletti, S., Neder, I., Rudner, M., Mahalu, D., Umansky, V. & Yacoby, A. 2011 Dephasing time of GaAs electron-spin qubits coupled to a nuclear bath exceeding 200 μs. *Nat. Phys.* **7**, 109–113. (doi:10.1038/nphys1856)

65 Ajoy, A., Álvarez, G. A. & Suter, D. 2011 Optimal pulse spacing for dynamical decoupling in the presence of a purely dephasing spin bath. *Phys. Rev. A* **83**, 032303. (doi:10.1103/PhysRevA.83.032303)

66 Naydenov, B., Dolde, F., Hall, L. T., Shin, C., Fedder, H., Hollenberg, L. C. L., Jelezko, F. & Wrachtrup, J. 2011 Dynamical decoupling of a single-electron spin at room temperature. *Phys. Rev. B* **83**, 081201. (doi:10.1103/PhysRevB.83.081201)

67 Souza, A. M., Álvarez, G. A. & Suter, D. 2012 Effects of time reversal symmetry in dynamical decoupling. *Phys. Rev. A* **85**, 032306. (doi:10.1103/PhysRevA.85.032306)

68 Jenista, E. R., Stokes, A. M., Branca, R. T. & Warren, W. S. 2009 Optimized, unequal pulse spacing in multiple echo sequences improves refocusing in magnetic resonance. *J. Chem. Phys.* **131**, 204510. (doi:10.1063/1.3263196)

69 Bylander, J. *et al.* 2011 Noise spectroscopy through dynamical decoupling with a superconducting flux qubit. *Nat. Phys.* **7**, 565–570. (doi:10.1038/nphys1994)

70 Almog, I., Sagi, Y., Gordon, G., Bensky, G., Kurizki, G. & Davidson, N. 2011 Direct measurement of the system–environment coupling as a tool for understanding decoherence and dynamical decoupling. *J. Phys. B* **44**, 154006. (doi:10.1088/0953-4075/44/15/154006)

71 Alvarez, G. A. & Suter, D. 2011 Measuring the spectrum of colored noise by dynamical decoupling. *Phys. Rev. Lett.* **107**, 230501. (doi:10.1103/PhysRevLett.107.230501)

72 Taylor, J. M., Cappellaro, P., Childress, L., Jiang, L., Budker, D., Hemmer, P. R., Yacoby, A., Walsworth, R. & Lukin, M. D. 2008 High-sensitivity diamond magnetometer with nanoscale resolution. *Nat. Phys.* **4**, 810–816. (doi:10.1038/nphys1075)

73 Meriles, C. A., Jiang, L., Goldstein, G., Hodges, J. S., Maze, J., Lukin, M. D. & Cappellaro, P. 2010 Imaging mesoscopic nuclear spin noise with a diamond magnetometer. *J. Chem. Phys.* **133**, 124105. (doi:10.1063/1.3483676)

74 Hall, L. T., Hill, C. D., Cole, J. H. & Hollenberg, L. C. L. 2010 Ultrasensitive diamond magnetometry using optimal dynamic decoupling. *Phys. Rev. B* **82**, 045208. (doi:10.1103/PhysRevB.82.045208)

75 de Lange, G., Ristè, D., Dobrovitski, V. V. & Hanson, R. 2011 Single-spin magnetometry with multipulse sensing sequences. *Phys. Rev. Lett.* **106**, 080802. (doi:10.1103/PhysRevLett.106.080802)

76 Khodjasteh, K. & Viola, L. 2009 Dynamically error-corrected gates for universal quantum computation. *Phys. Rev. Lett.* **102**, 080501. (doi:10.1103/PhysRevLett.102.080501)

77 Khodjasteh, K., Lidar, D. A. & Viola, L. 2010 Arbitrarily accurate dynamical control in open quantum systems. *Phys. Rev. Lett.* **104**, 090501. (doi:10.1103/PhysRevLett.104.090501)

78 West, J. R., Lidar, D., Fong, B. H. & Gyure, M. F. 2010 High fidelity quantum gates via dynamical decoupling. *Phys. Rev. Lett.* **105**, 230503. (doi:10.1103/PhysRevLett.105.230503)

79 Ng, H. K., Lidar, D. A. & Preskill, J. 2011 Combining dynamical decoupling with fault-tolerant quantum computation. *Phys. Rev. A* **84**, 012305. (doi:10.1103/PhysRevA.84.012305)

80 Boixo, S. & Somma, R. D. 2008 Parameter estimation with mixed-state quantum computation. *Phys. Rev. A* **77**, 052320. (doi:10.1103/PhysRevA.77.052320)

81 Khodjasteh, K. & Lidar, D. A. 2007 Performance of deterministic dynamical decoupling schemes: concatenated and periodic pulse sequences. *Phys. Rev. A* **75**, 062310. (doi:10.1103/PhysRevA.75.062310)

82 Hodgson, T. E., Viola, L. & D'Amico, I. 2010 Towards optimized suppression of dephasing in systems subject to pulse timing constraints. *Phys. Rev. A* **81**, 062321. (doi:10.1103/PhysRevA.81.062321)

83 Uhrig, G. S. & Lidar, D. A. 2010 Rigorous bounds for optimal dynamical decoupling. *Phys. Rev. A* **82**, 012301. (doi:10.1103/PhysRevA.82.012301)

84 Ng, H. K., Lidar, D. A. & Preskill, J. 2011 Aperiodic dynamical decoupling sequences in the presence of pulse errors. *Phys. Rev. A* **84**, 012305. (doi:10.1103/PhysRevA.84.012305)

85 Abragam, A. 1961 *Principles of nuclear magnetism*. London, UK: Oxford University Press.

86 Hanson, R., Kouwenhoven, L. P., Petta, J. R., Tarucha, S. & Vandersypen, L. M. K. 2007 Spins in few-electron quantum dots. *Rev. Mod. Phys.* **79**, 1217–1265. (doi:10.1103/RevModPhys.79.1217)

87 Kane, B. E. 1998 A silicon-based nuclear spin quantum computer. *Nature* **393**, 133–137. (doi:10.1038/30156)

88 Haeberlen, U. 1976 *High resolution NMR in solids: selective averaging*. New York, NY: Academic Press.

89 Magnus, W. 1954 On the exponential solution of differential equations for a linear operator. *Commun. Pure Appl. Math.* **7**, 649–673. (doi:10.1002/cpa.3160070404)

90 Cywinski, L., Lutchyn, R. M., Nave, C. P. & DasSarma, S. 2008 How to enhance dephasing time in superconducting qubits. *Phys. Rev. B* **77**, 174509. (doi:10.1103/PhysRevB.77.174509)

91 Uhrig, G. S. 2008 Exact results on dynamical decoupling by π pulses in quantum information processes. *New J. Phys.* **10**, 083024. (doi:10.1088/1367-2630/10/8/083024)

92 Pasini, S. & Uhrig, G. S. 2010 Optimized dynamical decoupling for power-law noise spectra. *Phys. Rev. A* **81**, 012309. (doi:10.1103/PhysRevA.81.012309)

93 Garroway, A. N. 1977 Homogeneous and inhomogeneous nuclear spin echoes in organic solids: adamantane. *J. Magn. Reson.* **28**, 365–371. (doi:10.1016/0022-2364(77)90276-1)

94 Kofman, A. G. & Kurizki, G. 2001 Universal dynamical control of quantum mechanical decay: modulation of the coupling to the continuum. *Phys. Rev. Lett.* **87**, 270405. (doi:10.1103/PhysRevLett.87.270405)

95 Uys, H., Biercuk, M. J. & Bollinger, J. J. 2009 Optimized noise filtration through dynamical decoupling. *Phys. Rev. Lett.* **103**, 040501. (doi:10.1103/PhysRevLett.103.040501)

96 Pan, Y., Xi, Z. & Cui, W. 2010 Optimal dynamical decoupling sequence for the Ohmic spectrum. *Phys. Rev. A* **81**, 022309. (doi:10.1103/PhysRevA.81.022309)

97 Quiroz, G. & Lidar, D. A. 2011 Quadratic dynamical decoupling with nonuniform error suppression. *Phys. Rev. A* **84**, 042328. (doi:10.1103/PhysRevA.84.042328)

98 Kuo, W.-J. & Lidar, D. A. 2011 Quadratic dynamical decoupling: universality proof and error analysis. *Phys. Rev. A* **84**, 042329. (doi:10.1103/PhysRevA.84.042329)

99 Wang, X., Yu, C.-S. & Yi, X. 2008 An alternative quantum fidelity for mixed states of qubits. *Phys. Lett. A* **373**, 58–60. (doi:10.1016/j.physleta.2008.10.083)

100 Chuang, I. L. & Nielsen, M. A. 1997 Prescription for experimental determination of the dynamics of a quantum black box. *J. Mod. Opt.* **44**, 2455–2467. (doi:10.1080/09500349708231894)
101 Santyr, G. E., Henkelman, R. & Bronskill, M. J. 1969 Variation in measured transverse relaxation in tissue resulting from spin locking with the CPMG sequence. *J. Magn. Reson.* **79**, 28–44. (doi:10.1016/0022-2364(88)90320-4)
102 Levitt, M. H. 1996 Composite pulses. In *Encyclopedia of nuclear magnetic resonance* (eds D. M. Grant & R. K. Harris), pp. 1396–1411. New York, NY: Wiley.
103 Tycko, R., Pines, A. & Guckenheimer, J. 1985 Fixed point theory of iterative excitation schemes in NMR. *J. Chem. Phys.* **83**, 2775–2802. (doi:10.1063/1.449228)
104 Pryadko, L. P. & Quiroz, G. 2009 Soft-pulse dynamical decoupling with Markovian decoherence. *Phys. Rev. A* **80**, 042317. (doi:10.1103/PhysRevA.80.042317)
105 Uhrig, G. S. & Pasini, S. 2010 Efficient coherent control by sequences of pulses of finite duration. *New J. Phys.* **12**, 045001. (doi:10.1088/1367-2630/12/4/045001)
106 Pasini, S., Karbach, P. & Uhrig, G. S. 2011 High-order coherent control sequences of finite-width pulses. *Europhys. Lett.* **96**, 10003. (doi:10.1209/0295-5075/96/10003)
107 Levitt, M. H. 2008 Symmetry in the design of NMR multiple-pulse sequences. *J. Chem. Phys.* **128**, 052205. (doi:10.1063/1.2831927)
108 Levitt, M. H. 2002 Symmetry-based pulse sequences in magic-angle spinning solid-state NMR. In *Encyclopedia of nuclear magnetic resonance* (eds D. M. Grant & R. K. Harris), pp. 165–196. New York, NY: Wiley.
109 Bravyi, S. & Kitaev, A. 2005 Universal quantum computation with ideal Clifford gates and noisy ancillas. *Phys. Rev. A* **71**, 022316. (doi:10.1103/PhysRevA.71.022316)
110 Souza, A. M., Zhang, J. & Laflamme, R. 2011 Experimental magic state distillation for fault-tolerant quantum computing. *Nat. Commun.* **2**, 169. (doi:10.1038/ncomms1166)

Robust dynamical decoupling

Alexandre M. Souza, Gonzalo A. Álvarez and Dieter Suter

Phil. Trans. R. Soc. A 2012 **370**, 4748-4769
doi: 10.1098/rsta.2011.0355